Journal of the Nigerian Association of Mathematical Physics
Volume28, No. 1, **(***November, 2014***), pp 75 – 82**

Application of Scale Resolution Models for Iris Pattern Segmentations Based On Edge Detections

Lanlege, D.I [1], Adeboye, K.R[2], Yahaya Y.A[3] and Isah.A.[4]

[1]Department of Mathematics and Computer Science,
Ibrahim Badamasi Babangida University, Lapai. Nigeria
[2, 3, 4]Department of Mathematics/Statistics, Federal University of Technology, Minna-Nigeria

Abstract

This paper considers scale resolution models for iris pattern segmentations based on edge detections. Edges in images can be mathematically defined as local singularities. Until recently, the Fourier transform was the main mathematical tool for analysing singularities. However, the Fourier transform is global and as such not well adapted to local singularities and it is hard to find the location and spatial distribution of singularities with Fourier transforms. It shows how vibration could be further minimized in the improved Mixed Radix Algorithm, by deriving a numerical algorithm for noise minimization in signal processing systems for faster pattern recognition. It is also proved analytically that this derived algorithm for noise minimization converges.

Keywords: Scale Resolution Model, Pattern Segmentation, Edge Detection, Singularities and Fourier Transform.

1.0 Introduction

A very common source of degradation in a digital image is noise contamination. Noise may be present in an image due to different reasons and its effect in degrading the image is different for different kinds of noise. The image corrupted with noise generally suffer from having low signal-to-noise ratio and may not be suitable for further processing without removing or reducing the effect of noise in it. For example, a biomedical image corrupted with noise cannot be used reliably for clinical diagnosis of disease. A satellite image corrupted with speckle noise fails to represent the remote-sensed data of, say, a geographical terrain. Hence removal of noise from the image is of utmost importance in image processing and analysis.
However, removal of noise like every known noise cleaning algorithm is associated with partial removal of the desired signal component. For example, mean filters generally blur the edges and the comer points present in the image.
Signature recognition is defined as the process of verifying the writer's identity by checking his/her signature against samples kept in a database. The result of this process is usually a number between 0 and 1 which represents a fit ratio (1 for match and 0 for mismatch). The threshold used for the confirmation/rejection decision depends on the nature of the application. The distinctive biometric patterns of this modality are the personal rhythm, acceleration and pressure flow when a person types a specific word or group of words (usually the hand signature of the individual).
This paper is aimed applying scale resolution models that will enable us carry out Iris Pattern Segmentations based on edge detections. The general mathematical construct is:

$$\frac{1}{\pi\left(r_i^2 - r_p^2\right)}\int_0^{\pi/2}\int_{r_p}^{r_i}\left(\frac{\delta}{r}\right)sin(\theta)rdrd\theta = \frac{4}{\pi}\frac{\delta}{r_i + r_p} \qquad (1)$$

Some of the methods and the results in edge detection are:

2.0 Edge Detector Using Wavelets

Wavelet transforms provide a local analysis; they are especially suitable for time-frequency analysis[1] such as for singularity detection problems. With the growth of wavelet theory, the wavelet transforms have been found to be remarkable mathematical tools to analyse the singularities including the edges, and further, to detect them effectively. Mallat *et al*. [2] proved that the maxima of the wavelet transform modulus can detect the location of the irregular structures. The wavelet

Corresponding author: ***Lanlege, D.I,*** E-mail: loislanlege@yahoo.com, Tel.: +2348030528667, +2348156073449

transform characterises the local regularity of signals by decomposing them into elementary building blocks that are well localised both in space and frequency. This not only explains the underlying mechanism of classical edge detectors, but also indicates a way of constructing optimal edge detectors under specific working conditions.

A remarkable property of the wavelet transform is its ability to characterise the local regularity of functions. For an image $f(x,y)$, its edges correspond to singularities of $f(x,y)$, and thus are related to the local maxima of the wavelet transform modulus. Therefore, the wavelet transform can be used as an effective method for edge detection.

Assume $f(x,y)$ is a given image of size $M \times N$ .At each scale j with $j > 0$ and $S_0 f = f(x,y)$ the wavelet transform decomposes $S_{j-1}f$ into three wavelet bands: a low-pass band $S_j f$, a horizontal high-pass band $W_j^H f$ and a vertical high-pass band.

$W_j^V f$ The three wavelet bands ($S_j f\ W_j^V f\ W_j^H f$) at scale j are of size $M \times N$, which is the same as the original image, and all filters used at scale j ($j > 0$) are up sampled by a factor of 2^jcompared with those at scale zero. In addition, the smoothing function used in the construction of a wavelet reduces the effect of noise. Thus, the smoothing step and edge detection step are combined together to achieve the optimal result. The short coming of this method is that the smoothing wavelet to reduce Noise cannot effectively remove the noise and Occlusion of the eye and this makes it difficult to segment Iris.

3.0 Filter Bank Gabor

The processing of facial images by a Gabor filter has been widely used for its biological relevance and technical properties. The Gabor filter kernels have similar shapes as the receptive fields of simple cells in the primary visual cortex. They are Multiscale and multi-orientation kernels. The Gabor transformed face images yield features that display scale, locality and differentiation properties. These properties are quite robust to variability of face image formation, such as the variations of illumination, head rotation and facial expressions.

4.0 Gabor Functions and Wavelets

The two-di1mensional Gabor Wavelets function $g(x,y)$and its Fourier transform $G(u,v)$ can be defined as follows:

$$G(x,y)\frac{1}{2\pi\sigma_x\sigma_y}\ell XP\left[-\frac{1}{2}\left(\frac{X^2}{\sigma_X^2}+\frac{Y^2}{\sigma_Y^2}\right)+2\pi lwx\right] \quad (2)$$

$$G(\mu,v)=\ell XP\left[-\frac{1}{2}\left(\frac{(\mu-w)^2}{\sigma_\mu^2}+\frac{v^2}{\sigma_v^2}\right)\right] \quad (3)$$

Where $\sigma\mu=\frac{1}{2}\pi\sigma_x$ and $\sigma_v=\frac{1}{2}\pi\sigma y$. Gabor functions can form a complete but non-orthogonal basis set. Expanding a signal using this basis provides localised frequency description. A class of self-similar functions, referred to as Gabor wavelets in the following discussion, is now considered. Let $g(x,y)$ be the mother Gabor wavelet, then this self-similar filter dictionary can be obtained by appropriate dilations and rotations of $g(x,y)$ through the generating function:

$$g_{mn}(x,y)=a^{-m}G(x,y) \quad (4)$$

$$x=a^{-m}(x\,cos\theta+ysin\theta) \quad (5)$$

$$y=a^{-m}(-x\,sin\theta+ycos\theta) \quad (6)$$

Where$a>1, m, n = integer\ and\ \theta = n\pi/k$ is the orientation (k is the number of orientations) and a^{-m} is the scale factor.

5.0 Gabor Filter Dictionary Design

The non-orthogonality of the Gabor wavelets implies that there is redundant information in the filtered images, and the following strategy is used to reduce this redundancy.

Let U_i and $U_h$denote the lower and upper centre frequencies of interest.

Let K be the number of orientations and S be the number of scales in the Multire solution decomposition. As proposed by [3] the design strategy is to ensure that the half-peak magnitude support of the filter responses in the frequency spectrum touch each other. This result in the following formulas for computing the filter parameters $\sigma\mu$and σv(and thus $\sigma x$and σy:

$$a=\left(\frac{U_h}{U_t}\right)^{-\frac{1}{s-1}} \quad (7)$$

$$\sigma_{mu}=\frac{(a-1)U_h}{(a+1)\sqrt{2In(2)}} \quad (8)$$

$$\sigma_v=tan\left(\frac{\pi}{2k}\right)\left[U_h-2In\left(\frac{2\sigma_\mu^2}{U_h}\right)\right]\left[2In(2)-\frac{[2In(2)]^2\sigma^2\mu}{U_h^2}\right] \quad (9)$$

where $W=U_h\ and\ m=0,1,\ldots S-1$.To eliminate the sensitivity of the filter response to absolute intensity values, the real (even) components of the $2D$Gabor filters are biased by adding a constant to make them zero mean.

6.0 Augmented Gabor-Face Vector

Given any image $I(x, y)$,its Gabor wavelet transformation is

$$W_{mn} = \int 1(x_1, y_1)\, g^*_{mn}(x - x_1, y - y_1)dx_1 dy_1 \quad (10)$$

Where g_{mn}indicates the complex conjugate of g_{mn}. The Gabor wavelet transformation of the facial image is calculated at S scales $m\epsilon\{0,1,2, \dots S\}$and K different orientations, $n\epsilon\{0,1,2, \dots K\}$and let us set$U_1 = 0.05$ and $U_h = 0.4$.

W_{mn}denotes a Gabor wavelet transformation of a face image at the scale m and orientation n. shows a sample face image from the database and its forty filtered images (five scales: $S = 5$ and eight orientations: $K = 8$have been taken).The augmented Gabor-face vector can then be defined as follows:

$$x = \left(W^t_{0,0\dots} W^t S_{,k}\right)^t \quad (11)$$

Where t is the transpose operator. The augmented Gabor-face vector can encompass all facial Gabor wavelet transformations, and has important discriminatory information that can be used in the classification step

7.0 The Conjugate Gradient Algorithm

The back propagation algorithm was the first and until recently the only algorithm to train feed forward multiplayer perceptrons. We here present the CGM variant.

Until recently, when the extended conjugate gradient method (ECGM) was formulated, the conjugate gradient method (CGM) has been one of the most effective method among the iterative methods for solving linear system of equations (of the form in equation(11) as a minimization method. The CGM provides faster convergence for quadratic functional than gradient descent methods while avoiding computation of the inverse of the Hessain matrix.

8.0 Materials and Methods

Since R is a positive definite, real symmetric n x n matrix, then the quadratic functional

$$F(W) = \frac{1}{2} w^T R w - w^T P + C \quad (12)$$

Has a unique minimum point w* which is a solution of the system of equations Qx=b.

Since $\nabla f(X) = \mathrm{Q_X} - \mathrm{b}$

Then we can write

$$\mathrm{Qx} * = \mathrm{b} \quad (13)$$

The minimization iteration updating method for (12) is given as

$$\mathrm{W_{k+1}} = \mathrm{W_k} + \alpha_\mathrm{k}(\mathrm{Rw_k} - \mathrm{P}) \quad (14)$$

Where

$$\alpha_\mathrm{k} = \frac{(\nabla \mathrm{f(x_k)})^\mathrm{T} \mathrm{d_k}}{\mathrm{d_k^T Q d_k}} \quad (15)$$

The value of the step size $\alpha_\mathrm{k}$that minimizes $f(X_{k+1})$ can be found by setting

$$\frac{df(x_k - \alpha_k(Qk_x - b))}{d\alpha_k} = O, \quad (16)$$

Yielding

$$\alpha_\mathrm{k} = \frac{(Qk_x - b)^T (Qk_x - L)}{(Qk_x - b)^T (Qk_x - b)} \quad (17)$$

With the step size α_k chosen as in equation (17), we have the following important result on the convergence rate of the gradient descent method.

9.0 The Active Contour Model

In active contour model, we use the technique of matching a deformable model to an image by means of energy minimization. An active contour model inhalized near the target refined iteratively and is attracted towards the salient contour. A snake in the image can be represented as a set of n points.

$$V_i = h(x_i, y_i) \quad (18)$$

Where $i = 0, \dots, n - 1$

We can write the energy function as:

$$\mathrm{E^*_{snake}} = \int_0^1 \mathrm{E_{in} V(S) ds} + \int_0^1 \mathrm{E_{image} V(S) ds} + \int_0^1 \mathrm{E_{con}\, V(S) ds} \quad (19)$$

$$\mathrm{E^*_{snake}} = \int_0^1 (\mathrm{E_{in}} + \mathrm{E_{image}} + \mathrm{E_{con}}) \mathrm{V(S) ds} \quad (20)$$

$$E_{ex} = E_{Image} + E_{con} \quad (21)$$

Where E_{in} denote internal energy of the spline (snakes) due to bending.
E_{image} denotes the image forces acting on spline
E_{con} denote external constraint force introduced by user
The combination of E_{image} and E_{con} can be represented asE_{ex}that denotes the external energy acting on the spline.
V(s) vector representing the spline
Internal energy of the snake as given by [4] is

$$E_{in} = E_{cont} + E_{cur}$$

Where E_{cont}denotes the energy of the snake contour.
E_{cur}denotes the energy of the spline curvature.
By finite difference notation:

$$\frac{dV}{ds} \approx V_{i+1} - V_i \quad (22)$$

$$\frac{d^2V}{ds^2} \approx (V_{i+1} - V_i) - (V_i - V_{i-1}) \quad (23)$$

$$= V_{i+1} - 2V_i + V_{i-1} \quad (24)$$

$$E_{in} = (\alpha(s)|V_S(s)|^2 + \beta(s)|V_{ss}(s)|^2)$$

$$E_{in} = \frac{\left(a(s)\left\|\frac{d\bar{v}}{ds}(s)\right\|^2 + \beta(s)\left\|\frac{d^2\bar{v}}{ds^2}(s)\right\|^2\right)}{2}$$

$$E_{in} = \sum_{i=0}^{n-1} \underbrace{\alpha(s)|V_{i+1} - V_i|^2}_{\text{Elasticity}} + \underbrace{\beta(s)|V_{i+1} - 2V_i + V_{i-1}|^2}_{\text{stiffness}}$$

Where α(s) regulates internal energy of the spline
β(s) regulates and develops the move curves of the spline
The first-order term makes the snake act like a membrane and second-order term makes it act like a thin plate. Large values of α(s) will increase the internal energy of the snake as it stretches more and more, whereas small value of α (s) will make the energy function insensitive to the amount of stretch. Similarly, large values of β(s) will increase the internal energy of the snake as it develops more curves, whereas small values of β (s) will make the energy function insensitive to curves in the snake. Smaller values of both α (s) and β (s) will place fewer constraints on the size and shape of the snake.
According [5], we introduce$(G_{x,y})$ as the gradient of the image and we have

$$E_{ex} = -\sum_i |G_x((x_i, y_i)|^2 + |G_y(x_i, y_i)|^2) \quad (26)$$

$$G_x = \frac{\partial}{\partial} G_\delta \otimes I \quad (27)$$

$$G_y = \frac{\partial}{\partial} G_\delta \otimes I \quad (28)$$Where $G(x, y)$ is the gradient image of the spline

We introduce the forward difference operator in order to move the gradient line to the region of interest.

$$E_{edge} = |\nabla(G(x, y) * I(x, y))|^2 \quad (29)$$

where

$$\nabla \equiv \left(\frac{\partial}{\partial x,}, \frac{\partial}{\partial y}\right) \quad (30)$$

and

$$G(x, y) = \frac{1}{\sqrt{2\pi\sigma^2}} e^{-\frac{(x - x_c)^2 + (y - y_c)^2}{2\sigma^2}} \quad (31)$$

$G(x, y)$ is a Gaussian smoothing function with scaling parameter σ to select the proper scale of edge analysis. The edge map is then used in a voting process to maximize the defined Hough transform.

$$H(x_c, y_c, r) = \sum_{i=1}^{n} h(x_i, y_i x_c, y_c, r) \quad (32)$$

As a standard image analysis tool used for finding curves that can be defined in a parametrical form such as lines and circles.[5] Maximum point in the Hough space corresponds to the radius r and centre coordinate x_c and y_c of the circle best defined by the edge points
$(x_i, y_i) \forall i = 1, \ldots, n$ (33)

$$H(x_c, y_c, r) = \sum_{i=1}^{n} h(x_i, y_i, x_c, y_c, r) \quad (34)$$

Where $H(x_c, y_c, r)$ shows a circle through a point, the coordinates of x_c, y_c, r define a circle

$$x_c^2 + y_c^2 + r^2 = 0 \quad (35)$$

For edge detection for iris boundaries the above equation becomes

$$(x_i - x_c)^2 + (y_i - y_c)^2 - r^2 = 0 \quad (36)$$

Simple Elastic Curve

For a curve represented as a set of points a simple elastic energy term is

$$E_{in} = \alpha(s) \sum_{i=0}^{n-1} L_i^2 \quad (37)$$

$$Ein = \alpha(s) \sum_{i=0}^{n-1} (x_{i+1} - x_i)^2 + (y_{i+1} - y_i)^2 \quad (38)$$

Where L_i^2 is the internal elastic component and α(s) control the internal elasticity of the curves

This makes the curve to shrink to a point (like a very small elastic band).

$$E_{total}(v_0, \cdots, v_{n-1}) = -\sum_{i=0}^{n-1} \|G(v_i)\|^2 + \alpha(s) \sum_{i=0}^{n-1} \|v_{i+1} - v_i\|^2 \quad (39)$$

$$E_{total}(v_0, \cdots, v_{n-1}) = \sum_{i=0}^{n-1} E_i(v_i, v_{i+1}) \quad (40)$$

Where $E_i(V_i, V_{i+1}) = -\|G(v_i)\|^2 + \alpha(s)\|v_{i+1} - v_i\|^2$

E_{total} can also be represented based on the concept of the expression derived by [6]

$$E_{total} = E_{in} + E_{ex} \quad (41)$$

Next, our work introduces$\alpha(s)$ as the strength of the internal elastic component which can be controlled, i.e

$$E_{in} = \alpha(s) \sum_{i=0}^{n-1} (L_i)^2 \quad or \quad (42)$$

$$E_{in} = \alpha(s) \sum_{i=0}^{n-1} L_i^2 \quad (43)$$

By dynamic programming, energy is minimized, that is43 is iterated until optimal position for each point in the centre of the iris i.e. the snake is optimal in the local search space constrained

$$E(V_1, V_2, \ldots, V_n,), = E_1(V_1, V_2) + E_2(V_2, V_3) + \ldots + E_{n-1}(V_{n-1}, V_n) \quad (44)$$

Curvature of level lies in a slightly smoothed image is used to detect corners and terminations in an image. Now,

$$\text{Let } C(x, y) = G\sigma * I(x, y) \quad (45)$$

be a slightly smoothened version of the image.

C = curvature of the image

$Let\ \theta = tan^{-1}\left(\frac{C_y}{C_x}\right)$ be the gradient of the image, where C_x and C_y are the coordinates of the pupil.

$\theta =$ Angle between the images of the curvatures

And let n = (cos θ, sinθ) be unit vector along the gradient direction

$\frac{dn}{d\theta}$= (- sinθ, cosθ) be unit vector along the perpendicular to the gradient direction.

The termination function energy E_{term} is represented by

$$E_{term} = \frac{d\theta}{dn} \quad (46)$$

$$E_{term} = \frac{d\theta}{dn} = \frac{d^2C/d^2n}{dC/dn} = \frac{C_{yy}C_x^2 - 2C_{xy}C_xC_y + C_{xx}C_y^2}{\left(C_x^2 + C_y^2\right)^{3/2}} \quad (47)$$

Constraint energy of some system, including the original snakes' implementation, allowed for user interaction to guide the snakes, not only in initial placement but also in their energy terms. Such constraint energy E_{con} can be used to interactively guide the snakes towards or away from particular features

Illustration

Find the area enclosed by the curve $r = 1 + cos\theta$ and the radius vectors at $\theta = 0\ and\ \theta = \pi/2$

$$A = \frac{1}{2}\int_0^{\pi/2} r^2\, d\theta = \frac{1}{2}\int_0^{\pi/2} (1 + 2cos\theta\ + cos^2\theta)d\theta \quad (48)$$

$$= \frac{1}{2}\left[\theta + 2sin\theta + \frac{\theta}{2} + \frac{sin2\theta}{4}\right]_0^{\pi/2} \quad (49)$$

$$= \frac{1}{2}\left\{\left(\frac{3\pi}{4} + 2 + 0\right) - (0)\right\} \quad (50)$$

$$\therefore = \frac{3\pi}{8} + 1 = 2.178 \quad (51)$$

So the area of a polar sector is easy enough to obtain. It is simply

$$A = \int_{\theta_1}^{\theta_2} \frac{1}{2} r^2 d\theta \quad (52)$$

To find the volume generated when the plane figure bound by $r = f(\theta)$ and the radius vectors at $\theta = \theta_1$ and $\theta = \theta_2$, rotates about the initial line.

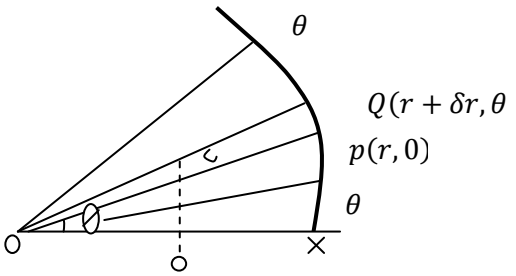

Figure 1 The volume of plane figure bounded by the polar curve

If we regard the elementary sector OPQ as approximately equal to the ∇OPQ the centroid C is distance 2r/3 from O.

We have: Area $OPQ \approx \frac{1}{2}r(r + \delta r)sin\delta\theta$

Volume generated when OPQ rotates about $OX = \delta V$

$\therefore \delta V$= area OPQ x distance travelled by its centroid (Pappus)

$$= \frac{1}{2}r(r + \delta r)sin\delta\theta.\, 2\pi.\text{CD} \quad (53)$$

$$= \frac{1}{2}r(r + \delta r)sin\delta\theta.\, 2\pi.\frac{2}{3}rsin\theta = \frac{2}{3}\pi r^2(r + \delta r)sin\delta\theta.\, sin\theta \quad (54)$$

$$\therefore \frac{\delta V}{\delta\theta} = \frac{2}{3}\pi r^2(r + \delta r)\frac{sin\delta\theta}{\delta\theta}.\, sin\theta \quad (55)$$

Then when $\delta\theta \to 0, \frac{dV}{d\theta} =$

56

$$V\ = \frac{2\pi r^2}{3}\int_{\theta_1}^{\theta_2} sin\theta d\theta \quad (57)$$

$$V = \frac{2\pi r^2}{3} cos\theta \Big|_{\theta_1}^{\theta_2} \quad (58)$$

Correct. This is another standard result.

To find the length of arc of the polar curve r = f(θ) between $\theta = \theta_1$and $\theta = \theta_2$

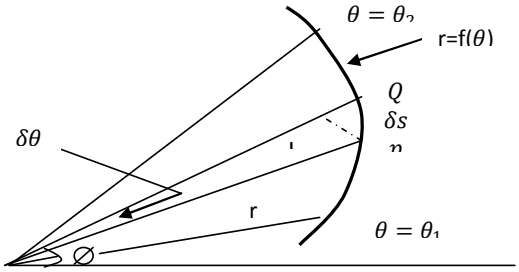

Figure 2 The length of arc of the polar curve

With the usual figure $\delta s^2 \approx r^2.\delta\theta^2 + \delta r^2 \therefore \frac{\delta s^2}{\delta\theta^2} \approx r^2 + \frac{\delta s^2}{\delta\theta^2}$ (3) (59)

$$if\,\delta\theta \to 0, \left(\frac{ds}{d\theta}\right)^2 = r^2 + \left(\frac{ds}{d\theta}\right)^2 \quad (60)$$

$$\therefore \frac{ds}{d\theta}\sqrt{r^2 + \left(\frac{ds}{d\theta}\right)^2} \quad (61)$$

$$s = \int_{\theta_2}^{\theta_2} \sqrt{r^2}\left(\frac{ds}{d\theta}\right)^2 d\theta \quad (62)$$

In their effort to find a good criterion for characterizing what the "best" function u should be, [6] sort for a criterion to minimize, which corresponds better to the structure of the images. They proposed the consideration of the "Bounded Variation" of the function u as a measure of the optimality of an image. The criterion is approximately the integral $\int_\Omega |\nabla u(x)| dx$ The main advantage is that this integral can be defined for functions that have discontinuities along hyper surfaces (in 2-dimensional images, along 1-dimensional curves), and this is essential to get a correct representation of the edges in images to facilitate pattern recognition

The problem to solve is

$$\text{Minimize } \left\{\int_\Omega |\nabla u(x)| dx\right\} \quad (63)$$

We use the notion of $\Gamma-$ Convergence to propose a numerical approach for computing a solution [7]presents the symmetry consideration and by the centering theorem of Fourier transform, we have reinforced the fact that the pixel Number, $N = 2^L$where$L \in Z^+$, is best in terms of speed, for the FFT and the IFFT operations for image processing for pattern recognition. When N is not a positive integer power of 2, we have modified/ improved the Mixed Radix Algorithm by stretching N to the next integer power of 2, using our established rule for stretching i.e. 0's for even values of N and 1's for odd value of N .when compared with the MATLAB fft (N) operator, it clearly shows an improvement in speed, over the Mixed Radix Algorithm.

Refer [7]& [8] $\Gamma-$ convergence is a special notion of convergence that is adapted to variation problems. If one is looking for the minimizes of a function $F(X), x \in X$ (where X is some space) and wants to approximate it with minimizers(X_n) of approximate problem $\min_X \in X, F_n(X)$, One wonders when (X_n) converges to a minimizer of F? Considering the classical notion of limits of functions, only the uniform convergence seems suitable to handle this problem. However, this notion of convergence is far too strong for most applications.

10.0 Conclusion

In the application of image processing tools, an image is first passed through the PID low pass filter which allows the image intensity to be adjusted by the image intensity adjustment tools. Then, finally sobel edge detector is used to enhance the outline of the image. This order is necessary for the processing because sobel edge detector is very sensitive to noise and needs to be filtered out before the edge detector application. More so, since the gradient of the sobel edge detector is related to the change in intensity at the edge of an object, the image intensity adjustment is used to produce a higher contrast image. As image intensity adjustment can improve the intensity of the image as well as noise within the image, the noise must be filtered out before the intensity adjustment. [9] Proportional Integral Derivative Controller Filter (PID) is employed to reduce the effect of noise.The new Multiscale Approach method for edge detection was able to detect iris region (pupil, outer boundary circle) using Snake Active Contour and Standard Galerkin Method. This in turn greatly reduces the search for the Hough transform, thereby improving the overall performance.

11.0 Recommendations

The Snake method introduces a Multiscale approach for edge detection by using active Contour model for efficiently detecting the iris region for use in the future extraction stage. Once this is done, a combined feature extraction scheme using Mat-lab algorithm components to extract all texture information from orientation in horizontal and vertical details is employed to obtain useful results.

References

[1] Goswami, M. K. (1999). Constrained Image Restoration and the Recovery of Discontinuities. IEEE Transition. PAMI, 3 (14), 367 – 383.

[2] Mallat, S. & Zhong, S.(1992) Analysis and Machine Characterization of Signal from Multiscale 710-732.

[3] Manjunath & Ma,L. (2003). Personal Identification Based on Iris Texture Analysis *IEEE Transaction on Pattern Analysis and Machine Intelligence*(25), 1519-1533

[4] Laurent, J.C. & Cohen, A.K. (2011). *Fundamentals of Wavelet: Theory, Algorithms, and Application.* New York, John Wiley& Sons, 409-431.

[5] Kong,W &Zhang, D (2001).Accurate Iris Segmentation Based on Novel Reflection And Eyelash Detection Model Proceeding of 2001 International Symposium on Intelligent Multi-Media,Video and Speech Processing Hong Kong in China

[6] Rudin L., Osher S. J. & Fatemi E. (1992). Nonlinear Total Variation Based Noise Removal Algorithms Physical D., 60, 259 – 268.

[7] Ezeako, (2005). Pattern Recognition: An Enhanced Sub-Array Algorithm for Processing of Large Data-Set Problems in a Transform Domain *Ph.D Thesis* Federal University OF Technology Minna 73-93.

[8] Adeboye, K. R. & Ezeako, L.N. (2007). Numerical Algorithm for Digital Image Enhancement and Noise Minimization, *Global Journal AS* 7 (1), 63-68

[9**]** Adeboye, K. R., Yahaya, Y. A. & Lanlege, D. I. (2013). Effective way of Noise Smoothing During Image Processing Using Multiscale Proportional Integral Derivative (PID) Filter Controller. *International Research Journal Science and Engineering T*echnology 2(2), 17-24.

[10] Adeboye, K. R., Lanlege D. I. & Gana, U. M. (2013). Musculoskeletal Magnetic Resonance Imaging Segmentation Using Finite Element Method *Journal of Nigeria Association of Mathematical Physics* 25(2), 65-72